NEOPLASIA
www.neoplasia.com

Volume 15 Number 11 November 2013 pp. 1231–1240 1231

Identification of Molecular Tumor Markers in Renal Cell Carcinomas with TFE3 Protein Expression by RNA Sequencing[1,2]

Dorothee Pflueger*,†,‡, Andrea Sboner§,¶, Martina Storz*, Jasmine Roth*, Eva Compérat#, Elisabeth Bruder, Mark A. Rubin§, Peter Schraml* and Holger Moch***

*Institute of Surgical Pathology, University Hospital Zurich, Zurich, Switzerland; †Life Science Zurich PhD Program on Molecular and Translational Biomedicine, Zurich, Switzerland; ‡Competence Center for Systems Physiology and Metabolic Diseases, Zurich, Switzerland; §Department of Pathology and Laboratory Medicine, Weill Cornell Medical College, New York, NY; ¶Institute for Computational Biology, Weill Cornell Medical College, New York, NY; #Department of Pathology, Pitié-Salpêtrière Hospital, Paris, France; **Institute of Pathology, University Hospital Basel, Basel, Switzerland

Abstract

TFE3 translocation renal cell carcinoma (tRCC) is defined by chromosomal translocations involving the *TFE3* transcription factor at chromosome Xp11.2. Genetically proven *TFE3* tRCCs have a broad histologic spectrum with overlapping features to other renal tumor subtypes. In this study, we aimed for characterizing RCC with TFE3 protein expression. Using next-generation whole transcriptome sequencing (RNA-Seq) as a discovery tool, we analyzed fusion transcripts, gene expression profile, and somatic mutations in frozen tissue of one *TFE3* tRCC. By applying a computational analysis developed to call chimeric RNA molecules from paired-end RNA-Seq data, we confirmed the known *TFE3* translocation. Its fusion partner *SFPQ* has already been described as fusion partner in tRCCs. In addition, an RNA read-through chimera between *TMED6* and *COG8* as well as *MET* and *KDR* (*VEGFR2*) point mutations were identified. An *EGFR* mutation, but no chromosomal rearrangements, was identified in a control group of five clear cell RCCs (ccRCCs). The *TFE3* tRCC could be clearly distinguished from the ccRCCs by RNA-Seq gene expression measurements using a previously reported tRCC gene signature. In validation experiments using reverse transcription–PCR, *TMED6-COG8* chimera expression was significantly higher in nine *TFE3* translocated and six TFE3-expressing/non-translocated RCCs than in 24 ccRCCs ($P < .001$) and 22 papillary RCCs ($P < .05$-$.07$). Immunohistochemical analysis of selected genes from the tRCC gene signature showed significantly higher eukaryotic translation elongation factor 1 alpha 2 (*EEF1A2*) and Contactin 3 (*CNTN3*) expression in 16 *TFE3* translocated and six TFE3-expressing/non-translocated RCCs than in over 200 ccRCCs ($P < .0001$, both).

Neoplasia (2013) 15, 1231–1240

Abbreviations: AA, amino acid; ccRCC, clear cell renal cell carcinoma; CDS, coding DNA sequence; FISH, fluorescence *in situ* hybridization; IHC, immunohistochemistry; PE, paired-end; RCC, renal cell carcinoma; RNA-Seq, next-generation whole transcriptome sequencing; RT-PCR, reverse transcription–polymerase chain reaction; TMA, tissue microarray; tRCC, translocation renal cell carcinoma; VHL, von Hippel-Lindau

Address all correspondence to: Dorothee Pflueger, PhD, Institute of Surgical Pathology, University Hospital Zurich, Schmelzbergstr. 12, CH-8091 Zurich, Switzerland.
E-mail: dorothee.pflueger@usz.ch

[1]This work was funded by the Swiss National Science Foundation (grant 135792; H.M.) and a Matching Fund of the University Hospital Zurich (D.P.). M.A.R. serves as a consultant to Gen-Probe, Inc and Ventana Medical Systems, Inc. Gen-Probe and Ventana have not played a role in the design and conduct of the study; in the collection, analysis, or interpretation of the data; or in the preparation, review, or approval of the manuscript. The other authors disclose no potential conflicts of interest.
[2]This article refers to supplementary materials, which are designated by Tables W1 to W4 and are available online at www.neoplasia.com.
Received 29 August 2013; Revised 21 October 2013; Accepted 21 October 2013

DOI 10.1593/neo.131544

Introduction

Xp11 (*TFE3*) translocation carcinomas are a separate and rare entity of renal cell carcinoma (RCC). The frequency of such tumors is exceptionally high in children and young adults accounting for 20% to 75% among childhood RCCs [1]. In contrast, the frequency of Xp11 translocation carcinomas in RCCs (tRCC) of adults ranges between 1% and 5%. Still, adult Xp11 tRCCs outnumber the juvenile cases by far because RCC is generally more often occurring in the adult population (3%-5% *vs* ~0.25%). *TFE3* tRCCs are defined by chromosomal translocations involving the *TFE3* transcription factor gene located at chromosomal band Xp11.2. *TFE3* belongs to the same family of micropthalmia transcription factors as *MITF*, *TFEB*, and *TFEC* (see Table W1 for expanded gene names). The Xp11 translocations in RCC fuse *TFE3* to one of several reported partner genes including *ASPSCR1* (*ASPL*), *PRCC*, *NONO*, *SFPQ* (*PSF*), and *CLTC* [1]. *TFE3* translocations also occur in alveolar soft part sarcoma [2], perivascular epithelioid cell tumor [3], and epithelioid hemangioendotheliomas [4]. *TFE3* tRCCs frequently share common morphologic features with clear cell RCC (ccRCC) and papillary RCC (pRCC) such as voluminous clear cytoplasm arranged in alveolar or papillary-like structure. Additionally, they can resemble multilocular cystic RCC or collecting duct carcinoma because they sometimes present with cystic-like features or tubular growth pattern [1]. Psammomatous calcification is often indicative for *TFE3* rearrangements. This wide spectrum of histologic features emphasizes the need for additional diagnostic tools.

As severe ambiguity and restrictions apply to diagnosing *TFE3* tRCC solely based on morphology and TFE3 immunohistochemistry (IHC), a new conception of gold standard has emerged. A growing body of data clearly demonstrates the need for additional molecular analyses by fluorescence *in situ* hybridization (FISH), PCR, or other techniques [5–8].

Over the last decade, high-throughput technologies have contributed to major advances in cancer research. Next-generation sequencing technology has the ability to inspect both cancer genomes [9,10] and transcriptomes [11–13]. Several times, the technique has been successfully applied to identify novel tumor-specific biomarkers (i.e., mutations, polymorphisms, genomic rearrangements or mRNA splice isoforms, and so on). Although the numerous *TFE3* fusion genes and the microphthalmia transcription factor family have been extensively studied in the past, there is only limited knowledge on other molecular alterations in *TFE3* tRCC. Mutations of the von Hippel-Lindau (*VHL*) tumor suppressor gene, which is inactivated in about 80% of ccRCC, or other frequently mutated genes in ccRCC coding histone-modifying and chromatin-remodeling enzymes (e.g., *PBRM1* or *BAP1*) [14,15] have not been found in tRCC [16]. Camparo et al. [17] published an expression signature of 83 differentially expressed genes in four tRCCs compared to 68 reference tumor samples, including ccRCCs, pRCCs, chromophobe and urothelial RCCs, oncocytomas, and normal renal tissue.

In this study, we performed next-generation whole transcriptome sequencing (RNA-Seq) with the goal of identifying additional molecular diagnostic markers in *TFE3* tRCC. We subjected the RNA-Seq data to an algorithm (FusionSeq [18]) proven effectively in the detection of RNA chimeras and gene fusions in prostate cancer [13], evaluated new protein markers, and sought for point mutations in key cancer genes.

Materials and Methods

Patients

For RNA-Seq, frozen tissue of an *TFE3* tRCC stored in the biobank of the Institute of Surgical Pathology, University Hospital Zurich (Zurich, Switzerland) was selected. The control group included five fresh frozen ccRCCs. The clinicopathologic data of these cases are summarized in Table W2.

To validate RNA expression data, we studied a cohort of 16 *TFE3* translocation (FISH+/IHC+) and 6 TFE3-expressing/non-translocated (FISH–/IHC+) RCCs by IHC (Table 1). All these cases were diagnosed by experienced uropathologists or pediatric pathologists (H.M., E.C., and E.B.). The cases were collected at the University Hospital Zurich, the Pitié-Salpêtrière Hospital (Paris, France), and the University Hospital Basel (Basel, Switzerland). The diagnosis of these cases was based on morphologic criteria, TFE3 IHC, and FISH. TFE3

Table 1. Characteristics of 22 *TFE3* Translocation and TFE3-Expressing/Non-Translocated Cases.

Case No.	TFE3 IHC	*TFE3* FISH	Sex, Age	pT N M	Fuhrman Grade	Cohort	Comment
1	Positive	Positive	Female, 16	pT1b N1 Mx	2	Zurich	
2	Positive	Positive	Female, 77	pT1b Nx Mx	x	Zurich	Case 26 [28]
3	Positive	Positive	Female, 20	pT3a N1 M0	2	Zurich	
4	Positive	Positive	Female, 22	pT1a N0 M0	2	Zurich	
5	Positive	Positive	Female, 69	pT1b Nx Mx	x	Zurich	
6	Positive	Positive	Male, 8	pT3 N1 Mx	x	Zurich	
7	Positive	Positive	Female, 23	pT1b Nx Mx	2	Paris	
8	Positive	Positive	Female, 33	pT1a N1 Mx	2	Paris	
9	Positive	Positive	Female, 22	pT2 Nx Mx	3	Paris	
10	Positive	Positive	Male, 29	pT2 N0 Mx	3	Paris	
11	Positive	Positive	Female, 8	pTx Nx Mx	x	Basel	Case 5 [19], case 8 [20]
12	Positive	Positive	Male, 9	pTx Nx Mx	x	Basel	Case 7 [19], case 14 [20]
13	Positive	Positive	Female, 15	pTx Nx Mx	x	Basel	Case 8 [19], case 10 [20]
14	Positive	Positive	Male, 13	pTx Nx Mx	x	Basel	Case 12 [19]
15	Positive	Positive	Female, 11	pTx Nx Mx	x	Basel	Case 13 [19]
16	Positive	Positive	Female, 19	pTx Nx Mx	x	Basel	Case 11 [19]
17	Positive	Negative	Male, 41	pTx Nx M1	x	Zurich	
18	Positive	Negative	Male, 71	pT1b Nx Mx	3	Zurich	
19	Positive	Negative	Female, 55	pT1a Nx M0	3	Zurich	
20	Positive	Negative	Female, 54	pTx Nx Mx	x	Zurich	
21	Positive	Negative	Male, 57	pT1a Nx Mx	2	Paris	
22	Positive	Negative	Male, 87	pT3a Nx Mx	4	Paris	

expression was evaluated by IHC on whole block sections (TFE3, sc-5958; Santa Cruz Biotechnology, Heidelberg, Germany). Neoplasms showing moderate (2+) to strong (3+) nuclear labeling for TFE3 visible at low power (×4-10) and weak (1+) labeling appreciable only at high power (×20) in the absence of staining of normal tissues were considered positive. Neoplasms with no nuclear labeling (0+) were considered negative. Broad or focal cytoplasmic staining was not considered.

All 22 cases were assembled to a tissue microarray (TMA) on which each tumor was represented with two cores of 0.6-mm diameter and further analyzed for *TFE3* translocation by *TFE3* break-apart FISH (SPEC *TFE3* Dual Color Break Apart Probe; ZytoVision, Bremerhaven, Germany). Here, the tRCC index case served as a positive control. Evaluation of *TFE3* FISH signals was non-automated.

In addition, formalin-fixed paraffin-embedded (FFPE) tissue of 24 ccRCCs and 22 pRCCs was used for RNA extraction to perform TaqMan assays on RNA chimeras. Two TMAs with 390 renal tumors (274 ccRCCs, 25 type I pRCCs, 30 type II pRCCs, 18 chromophobe RCCs, 2 collecting ducts of Bellini, 16 unclassified RCCs, 3 Wilms tumors, and 22 oncocytomas) were used for marker protein expression study. These TMAs have been described in [19–21]. The study was approved by the Cantonal Ethics Committee of Zurich (KEK-ZH-Nr. 2001-0072/4).

RNA-Seq and Data Processing to Call Chimeric Transcripts

Sections (10 × 10 μm thick) were cut from frozen tumor blocks. RNA extraction was performed using TRIzol reagent (Life Technologies, Zug, Switzerland). RNA integrity was validated by 2100 Bioanalyzer (Agilent Technologies, Basel, Switzerland). Paired-end (PE) RNA-Seq was conducted at Prognosys Biosciences (La Jolla, CA) using the Genome Analyzer II from Illumina (San Diego, CA). Library preparation was done according to existing protocols [13] with the following parameters: 550-bp fragment length of the cDNA library and 50- to 100-bp read length. In total, 298 Mio reads were generated, of which 151 Mio (50.8%) reads were mapped to the human genome reference sequence (hg18) and a custom-generated splice junction library based on UCSC Known Genes annotation data set (Table W2). We allowed for up to two mismatches per read. We also discarded reads that could be aligned to more than five distinct locations in the genome. If a read could be mapped to up to five locations, the one with the best score (i.e., less number of mismatches) is selected. As part of a standardized RNA-Seq analysis procedure in the Gerstein Lab at Yale University [22], the data were made anonymous and genome-wide gene and exon expression values [reads per kilobase of the gene model per million mapped reads (RPKM)] were calculated for all six RCCs. The PE reads were then processed through FusionSeq. All steps in this analysis pipeline are described in detail by Sboner et al. [18]. In brief, the program aligns all reads to the human genome (hg18) and searches for PE reads where one read maps to gene A and the other read maps to gene B. After filtering out artifactual PE read alignments, it classifies remaining instances as interchromosomal, intrachromosomal, or cis-chromosomal rearrangements if gene A and gene B are located on different chromosomes, same chromosome/same orientation, or same chromosome/opposed orientation, respectively. PE reads mapping to two genes with the same orientation and located directly adjacent on the same chromosome were designated as read-through candidate. The software attributes confidence values to each candidate that enables for prioritization in validation experiments. Ratio of empirically computed supportive PE reads was used as the score to prioritize follow-up in this study.

Gene Expression Profiling from RNA-Seq Data

We calculated gene expression from RNA-Seq data as proposed by Mortazavi et al. [23]. All genome-wide RPKM values were quantile normalized. The composite exon model used here is described in detail elsewhere [18]. For gene expression analysis by RNA-Seq, we selected 80 genes from the renal translocation carcinoma signature published by Camparo et al. [17] and calculated the fold change expression in our tRCC compared to the mean expression level of the five ccRCCs. Three gene IDs from this signature could not be found in our gene list. Hierarchical clustering was done with the MultiExperiment Viewer (MeV; Dana-Farber Cancer Institute, Boston, MA). Significance ($P < .05$) was calculated by one-way analysis of variance (ANOVA) and Bonferroni correction.

Mutation Analysis Using RNA-Seq Data

DNA extraction was done with AllPrep DNA/RNA Mini Kit (Qiagen, Hilden, Germany) from 3 × 10 μm section of the same frozen tumor blocks used for RNA-Seq. We sought mutations in selected oncogenes and tumor suppressor genes with specific emphasis on critical players in RCC-specific pathways and/or genes frequently mutated in RCC [15,24]. The following 30 genes were selected: *EGFR*, *KIT*, *BRAF*, *KRAS*, *AKT1*, *PIK3CA*, *CCND1*, *CDK1*, *CDK2*, *TP53*, *PTEN*, *CDKN2A* (p16), *RB1*, *VHL*, *HIF1A*, *EPAS1* (*HIF2A*), *MET*, *MTOR*, *KDR* (*VEGFR2*), *FLT4* (*VEGFR3*), *KDM5C* (*JARID1C*), *KMT2D* (*MLL2*), *NBN*, *NF2*, *PMS1*, *SETD2*, *KDM6A* (*UTX*), *WRN*, *UBR4* (*ZUBR1*), and *PBRM1*. We inspected all reads covering the exons of 30 cancer genes using the Broad Institute's Integrated Genome Viewer (gene model hg18) and called base pair exchanges manually by applying the following criteria: 1) Only high-quality reads were considered. 2) Alterations in the two first or last positions of the reads were rejected (criterion based on [25]; error rates increase with read length, and high error rate for first bases in some of the reads may be due to a long first cycle processing time and lack of pre-phasing or interference of the first bases with parts of the adapter sequence). 3) A minimum of 10 covering reads (favorably stacked) and at least 35% reads harboring the base pair exchange (criterion set empirically to enrich high-frequency mutations). 4) Less than 10 covering reads were considered when 100% reads harbored the exchanged base pair (criterion set empirically). Base pair exchanges were compared to dbSNP (build 130) to filter out known polymorphisms. Remaining somatic mutations obtained from RNA-Seq were verified by PCR and subsequent sequencing on tumor DNA (for primer sequences, see Table W3). The positive hits were confirmed by a second independent PCR on tumor and normal DNA. The functional impact of missense protein mutations was evaluated using MutationAssessor (http://mutationassessor.org/; Memorial Sloan Kettering Cancer Center, New York, NY), which bases its assessment on evolutionary conservation of the affected amino acid (AA) in protein homologs. The method for detection of *VHL* mutations was reported in detail [26].

Validation of Chimeric Transcripts by Reverse Transcription–PCRs and Sanger Sequencing

cDNA was prepared using High Capacity cDNA Reverse Transcription Kit (Life Technologies) from the same RNA aliquot used

in RNA-Seq. Chimeric RNA was validated by PCR using at least two different primer pairs per candidate. The primers were located in exons encompassing the mRNA junction point of the two genes. Resulting PCR bands were gel purified and sequenced on a conventional ABI sequencer. Primer sequences are reported in Table W3.

TaqMan Assay for TMED6-COG8 *and* TFE3 *Expression Measurement*

RNA extraction from FFPE tissue was done as described [27] with the following modification: instead of cutting sections, three tissue cylinders (0.6-mm diameter) were punched from the tumor areas of the tissue blocks. The quantitative measurements were performed using the TaqMan RNA-to-Ct 1-step kit (Life Technologies) with 30 ng of RNA in each technical triplicate and the cycling parameters according to the protocol on a ViiA7 (Life Technologies). Primer and probe sequences for the TaqMan assays are given in Table W3.

Validation of Protein Markers by IHC

We selected *EEF1A2*, *MUC1*, *CNTN3*, *SV2B*, *NTSR2*, *TRIM63*, and *IGFN1* because these genes were significantly differentially regulated and antibodies suitable for paraffin IHC were available. For the putative *TFE3* translocation and TFE3-expressing/non-translocated RCC marker proteins SV2B (NBP1-46368; Novus Biologicals, Cambridge, United Kingdom), NTSR2 (LS-A1265; LifeSpan Biosciences, Seattle, WA and ab48273; Abcam, Cambridge, United Kingdom), TRIM63/MURF1 (AP16114PU-N; Acris, Herford, Germany), and DKFZp434B1231/IGFN1 (H91156-A01; Abnova, Heidelberg, Germany and HPA039566; Sigma, St Gallen, Switzerland), we were not able to establish working IHC procedures. IHC for EEF1A2 (Human Protein Atlas, sc68481, 1:50; Santa Cruz Biotechnology), MUC1 (NCL-MUC-1, clone Ma695, 1:50; Novocastra, Nunningen, Switzerland), and CNTN3 (Human Protein Atlas, NBP1-89971, 1:50; Novus Biologicals) revealed reliable results with breast cancer, normal lung, and normal uterus as positive controls, respectively. A three-graded system (0, negative; 1, weak/moderate; 2, strong) was used to measure protein expression. Statistical testing was done using a χ^2 test with a confidence interval of 95%.

Results

Identification of Fusion Transcripts

Each tumor sample displayed variant numbers of chimeric RNA candidates (Figure 1*A*). Interchromosomal, intrachromosomal, and cis-chromosomal candidates represent the best candidates for unraveling genomic rearrangements (see Materials and Methods section for definition). The most promising nine candidates were selected for validation (Figure 1*B*). The cis candidate turned out to be a false positive RNA chimera due to incomplete gene annotation as exemplified by another detailed description of a false positive cis chimera in prostate cancer [13]. *GATAD1* transcription extends to include exons in the gene region of *PEX1* (data not shown).

Among the intrachromosomal and interchromosomal candidates, solely the top candidate *SFPQ-TFE3* in our tRCC index case was verifiable. This 22-year-old patient presented with a renal tumor that exhibited histologic features of mixed clear cell/papillary structure and calcifications (psammoma bodies; Figure 2*A*). The tumor showed strong nuclear expression of TFE3 by IHC (Figure 2*B*) and a *TFE3* translocation by FISH (Figure 2*C*). In the RNA-Seq data, 112 PE reads connected exons of *SFPQ* to exons of *TFE3* (Figure 2*D*). Reverse transcription (RT)–PCR and sequencing confirmed the expression of an *SFPQ-TFE3* chimeric transcript (Figure 2*E*). RNA-Seq is also a useful tool for measuring exon-specific expression levels [23]. Because of the translocation event that places *TFE3* under the control of its 5′ partner's promoter, *TFE3* is overexpressed. In the tRCC, we show for both partner genes that exons within the gene fusion transcript have a significantly (P = .04) higher mean expression level than exons lost in the translocation event (Figure 2*E*). The remaining eight gene fusion candidates could not be validated by RT-PCR and represented false positives.

In the tRCC, we discovered an RNA read-through candidate joining exons of *TMED6* with *COG8*. *TMED6* was also identified in the Xp11 translocation carcinoma gene signature list, published by Camparo et al. [17]. We verified this candidate by RT-PCR and found three different isoforms of the *TMED6-COG8* (*TC*) chimera, all of them retaining an N-terminally truncated COG8 open reacting frame (Figure 3*A*). Compared to ccRCC, median *TC* levels were 1289-fold increased in *TFE3* tRCCs and 114-fold in TFE3-expressing/non-translocated

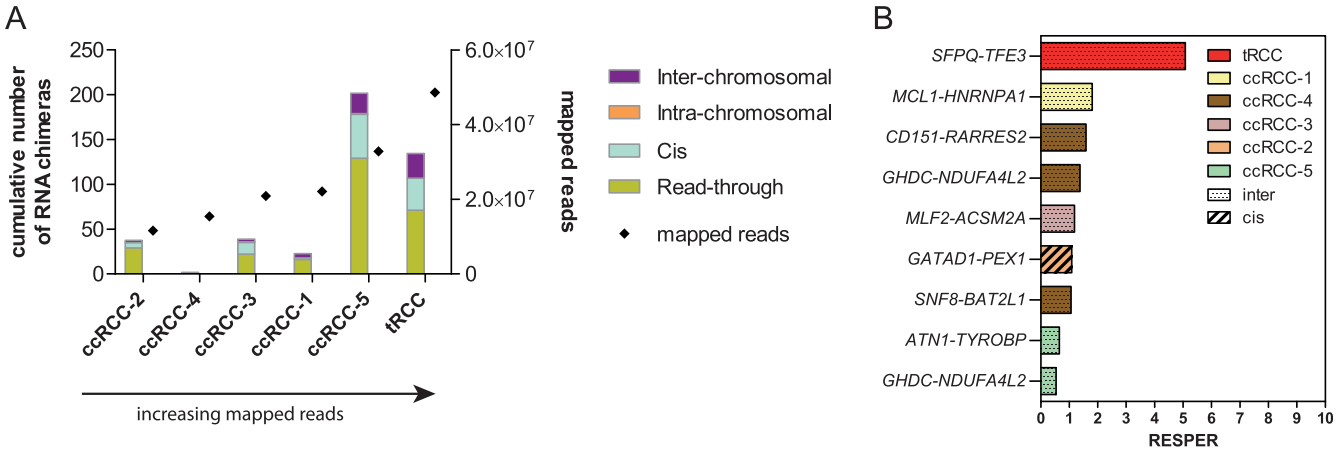

Figure 1. Overview of RNA chimera calls in six RCC samples. (A) Summary of all classes of RNA chimera calls from FusionSeq in all samples sorted by sequencing depth. (B) Nine top-scored interchromosomal/intrachromosomal and cis candidates selected for verification by RT-PCR.

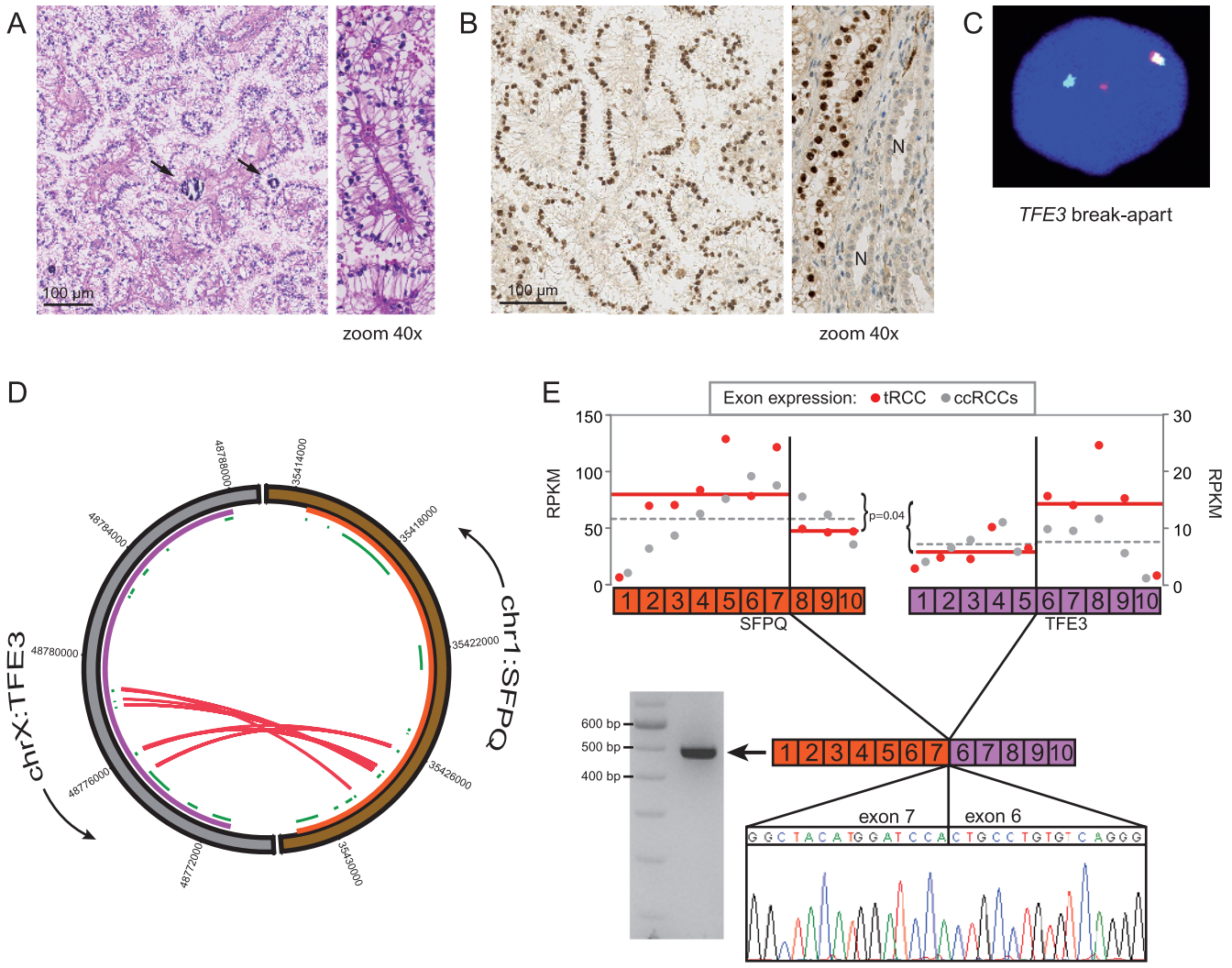

Figure 2. Identification of *SFPQ-TFE3* gene fusion in renal cancer. (A) Histology of the index *TFE3* tRCC case (left panel) with a zoom in on papillae of tumor cells with clear cytoplasm (right panel). Arrows indicate typical calcifications. (B) TFE3 IHC of tRCC (left panel) with the nuclei of cancer cells strongly stained. No staining of the nuclei of epithelial cells lining adjacent normal (N) renal tubules (right panel). (C) A representative cancer nucleus of tRCC displays *TFE3* rearrangement. The split of a yellow signal into distinct red and green signals marks a broken *TFE3* allele. The remaining yellow signal represents the remaining intact *TFE3* allele. (D) The circus image represents a zoom in on the genomic location of the *SFPQ* gene (orange) on chromosome 1 (brown) and the *TFE3* gene (purple) on chromosome X (gray). Exons are displayed in green. PE reads (red) connect *SFPQ* (NM_005066.2) 5′ exons to *TFE3* (NM_006521.4) 3′ exons. (E) The fusion transcript consists of *SFPQ* exons 1 to 7 and *TFE3* exons 6 to 10 (lower panel). Red dots represent the expression value per exon of the tRCC; gray dots represent the mean expression value per exon of the other five ccRCC samples combined. The lines mark the mean expression value of exons within the fusion transcript and exons lost in the fusion event. For both genes, these two groups of exons display a significant difference in expression in the translocation case (red lines) but not in the other RCCs (gray dotted lines).

RCCs (Figure 3*B*). Compared to pRCC, the up-regulation was still 22-fold in *TFE3* tRCC and 1.9-fold in TFE3-expressing/non-translocated RCC. Despite up-regulation of TFE3 at the protein level, overall *TFE3* RNA levels were not significantly altered among the RCC subgroups (Figure 3*C*).

Gene and Protein Expression Profiles

Using RNA-Seq and data from the recently published expression signature from Camparo et al., the tRCC displayed 48 upregulated signature genes, of which 41 (85%) were also overexpressed in the data set of Camparo et al. (Figure 4*A*). Thirty-two genes were down-regulated, of which 27 (84%) were in concordance with Camparo et al. Using this signature, we were able to clearly distinguish the tRCC from the five ccRCCs.

To further validate the signature at the protein level, we investigated the expression pattern of three putative marker proteins on a TMA. Sixteen cases were translocated and had strong/moderate nuclear TFE3 expression (termed "*TFE3* tRCC"; Table 1). We did not find *TFE3* genomic rearrangements in 6 of 22 (27%) cases displaying histologic features suggestive for *TFE3* translocation but with weak (n = 2), moderate (n = 2), or strong (n = 2) nuclear TFE3 immunoreactivity (termed "TFE3-expressing/non-translocated RCC"). The *TFE3* break-apart FISH assay was repeated on large sections of these latter six tumors to confirm the results from the

small TMA cores and to rule out tumor heterogeneity. Here, *TFE3* was not rearranged either.

EEF1A2 and *CNTN3* were chosen as marker genes overexpressed in *TFE3* tRCCs and *MUC1* as a downregulated gene. Loss of MUC1 expression is observed in *TFE3* tRCC (56%) but also in the common subtypes such as ccRCC (18%) and pRCC (21%), as well as in unclassified RCC (44%), chromophobe (6%), and oncocytomas (5%; Figure 4*B*). Strong EEF1A2 expression was seen in both *TFE3* translocation (88%) and TFE3-expressing/non-translocated RCCs (50%). Only a minor fraction of pRCC (15%) and ccRCC (1%), as well as unclassified RCC (10%) also had such strong expression of EEF1A2. CNTN3 expression was more diverse; although 19% *TFE3* tRCCs and 67% TFE3-expressing/non-translocated RCCs displayed strong CNTN3 expression compared to only 4% of ccRCC, levels were also high in the papillary subtype, oncocytomas, Wilms tumors, and unclassified RCC (14%-33%).

Mutation Analysis

To identify mutations using RNA-Seq data, we manually called base pair exchanges in the genes' coding sequences (CDSs) and untranslated regions. In total, we identified 288 base pair exchanges that met the criteria (see Materials and Methods section). Most of them (n = 263) were located in the CDS (Table 2). In the CDS, 220 (84%) were discarded as known single-nucleotide polymorphisms (SNPs) and 43 (16%) were further analyzed by RT-PCR and Sanger sequencing (green-labeled in Table W4). In the tRCC, we identified two heterozygous germline mutations in exon 2 of the *MET* gene and in exon 16 of the *KDR VEGFR2* gene. The G24E AA exchange in MET pertains to the N-terminal signal peptide region, whereas the A757G exchange of VEGFR2 is located in the extracellular domain. In ccRCC-5, we found a heterozygous, somatic [C/T] mutation in exon 23 of *EGFR* (Figure 5). The mutation is located in the tyrosine kinase domain of the EGFR, and MutationAssessor predicted a high functional impact of the R932C AA exchange.

Discussion

Using RNA-Seq, we discovered that high levels of the *TMED6-COG8* RNA read-through chimera and elevated expression of EEF1A2 and CNTN3 protein are potential molecular markers of *TFE3* translocation and TFE3-expressing/non-translocated RCCs. In addition, RNA-Seq allowed identification of *SFPQ* as fusion partner in a *TFE3* tRCC, as well as mutations in the therapeutically relevant genes *MET* and *VEGFR2*.

Our index case for *TFE3* translocation (tRCC) showed an *SFPQ-TFE3* gene fusion, which may not be as frequent as *ASPL-TFE3* or *PRCC-TFE3* fusions. For RCC, a minimum of 13 *PRCC-TFE3* and *ASPL-TFE3* fusions each is reported, as genetically confirmed in several studies [17,28–30]. A minimum of five RCC cases of genetically confirmed *SFPQ-TFE3* fusions exists in the literature [17,28,30]. Interestingly, five *SFPQ-TFE3* tRCCs were intermingled in a cohort of more than 400 histologically diagnosed ccRCC cases [16], demonstrating the difficult differential diagnosis between ccRCC and *TFE3* tRCC, because both tumor types share some morphologic features. *SFPQ-TFE3* fusions are also found in perivascular epithelioid cell tumors; the case reported by Tanaka et al. [31] located to the gastrointestinal tract and expressed a fusion transcript between *SFPQ* exon 7 and *TFE3* exon 5.

In our attempt to identify novel gene fusions in RCC, we were confronted with some low-score gene fusion candidates. Although we reconciled with the Mitelman Database of Chromosome Aberrations

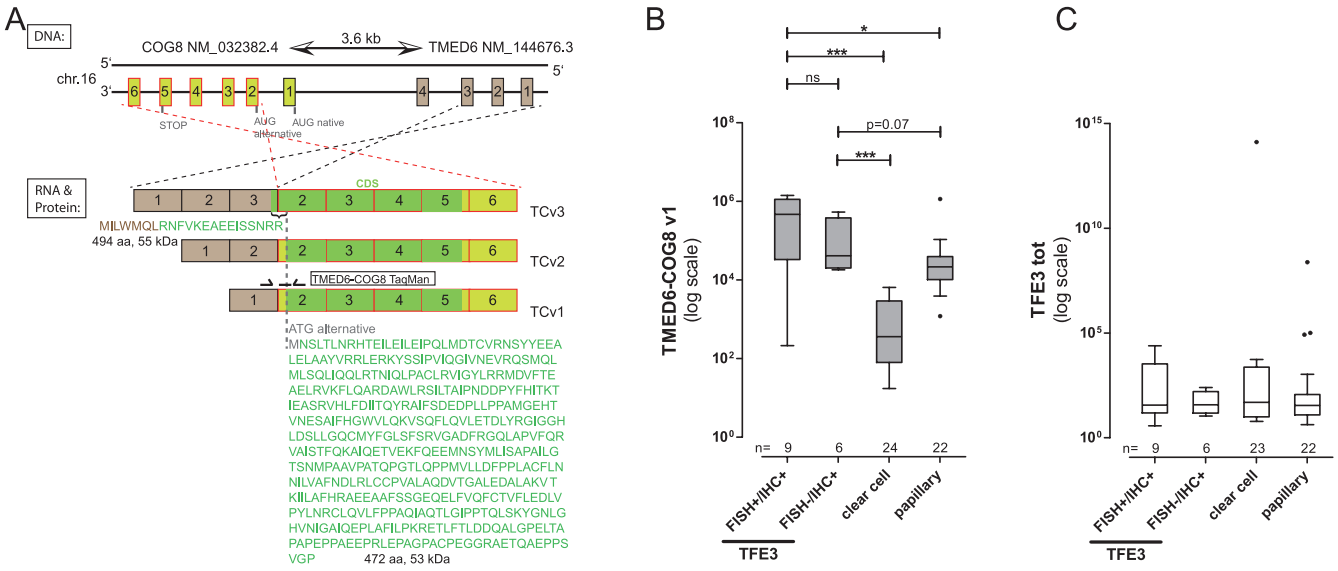

Figure 3. *TMED6-COG8* (*TC*) read-through in RCC. (A) DNA: Schematic representation of the genomic structure of *TMED6* and *COG8* on the DNA (−) strand. RNA: Three isoforms were expressed with *TCv1* being the prominent one. The TaqMan assay used to detect *TC* levels in RCCs is indicated. Protein: Two isoforms encode N-terminally truncated COG8 from an alternative ATG START sites downstream of the original one in *COG8* exon 1. The TCv3 isoform uses an ATG provided by the *TMED6* sequence. The COG8 CDS is given in green, and the small appendage on the N-terminus in TCv3 is given in brown. (B) *TMED6-COG8* (*TCv1*) levels were measured in FFPE samples of *TFE3* translocation (median expression at 467,735) and TFE3-expressing/non-translocated RCCs (at 41,210) and compared to ccRCCs (at 363) and pRCCs (at 21,627); ***P < .001 and *P < .05; ns, not significant. (C) Total *TFE3* expression encompassing the fusion transcripts measuring levels of exons 8 and 9.

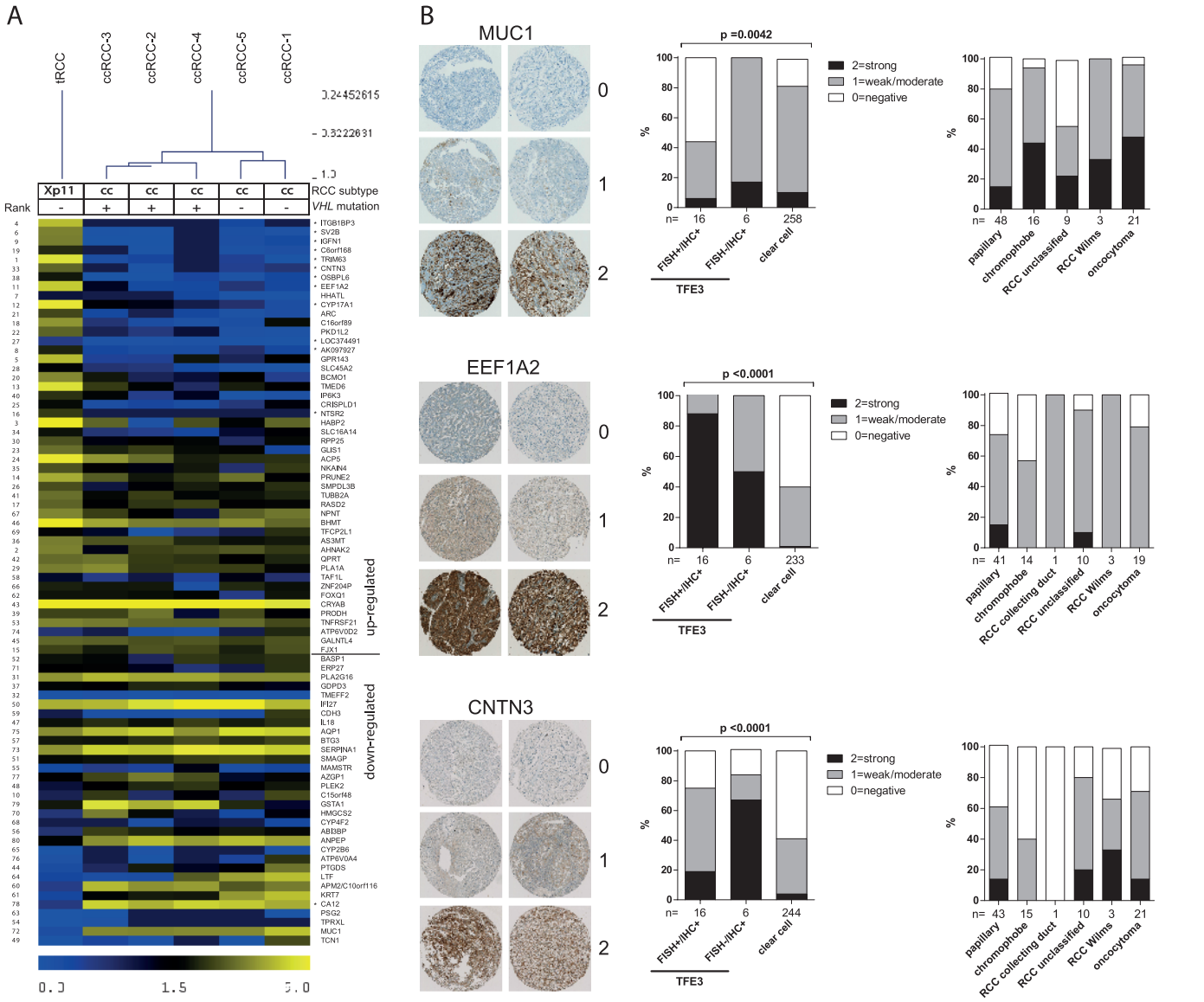

Figure 4. Gene expression profile from RNA-Seq data supports a known renal translocation signature. (A) The heat map is a representation of expression values of 80 signature genes. The genes are sorted according to their fold change expression difference between the tRCC and the mean value of the other five ccRCCs. Significant genes (corrected $P < .05$) are marked by asterisk. On the left, the genes were ranked according to fold change expression difference by Camparo et al. [17]. (B) Expression pattern of marker genes selected from A across different RCC subtypes. Significance was calculated by χ^2 test.

and Gene Fusions in Cancer (http://cgap.nci.nih.gov/Chromosomes/Mitelman), we found none of these partner genes involved in genomic rearrangements in renal or other cancer types. This and their low probability score indicate them as artificial candidates likely generated during library preparation. This is also consistent with the recent data from the Cancer Genome Atlas Research Network, which did not report any new chromosomal rearrangements in 400 ccRCCs [16].

Importantly, we identified *TMED6-COG8* (*TC*) as a novel RNA read-through molecule with elevated expression in *TFE3* translocation and TFE3-expressing/non-translocated RCCs. RNA read-throughs

Table 2. Base Pair Exchange Calls in RNA-Seq Data.

	tRCC		ccRCC-1		ccRCC-2		ccRCC-3		ccRCC-4		ccRCC-5		Total	
	n	%	*n*	%	*n*	%	*n*	%	*n*	%	*n*	%	*N*	%
Total	68		61		23		37		50		49		288	
Untranslated region	2	3	9	15	1	4	2	5	8	16	3	6	25	9
CDS	66	97	52	85	22	96	35	95	42	84	46	94	263	91
SNP	60	91	38	73	20	91	29	83	29	69	44	96	220	84
No SNP	6	9	14	27	2	9	6	17	13	31	2	4	43	16

are evolving as a novel class of tumor markers, an example being *SLC45A3-ELK4* in prostate cancer [32,33]. It was regarded as an important finding because it is the first description of an RNA read-through detectable in urine of patients with prostate cancer due to its hormone-dependent overexpression. The elevated expression of *TC* may point to a potential diagnostic marker for *TFE3* tRCCs, because *TCv1* expression was significantly higher in *TFE3* tRCCs compared to ccRCC and pRCC in our TaqMan assay. *TMED6* is highly expressed in α cells of the pancreatic islets and is associated with insulin production and secretion [34]. COG8 is part of a multiprotein complex in the Golgi apparatus and responsible for intracellular trafficking and protein glycosylation [35]. It is possible that the read-through event with *TMED6* leads to an up-regulation of an N-terminally truncated COG8 protein. We can only hypothesize about its function in RCC. *TC* read-through may prove detectable at the RNA level not only in tissue but also in urine, blood, or circulating tumor cells of patients with *TFE3* tRCC. Moreover, up-regulation of *TC* levels also in TFE3-expessing/non-translocated RCCs suggests a common biologic mechanism shared with *TFE3* tRCCs.

Using RNA-Seq and data from the recently published expression signature [17], we were able to separate our tRCC from ccRCCs, implying that the list of differentially expressed genes by Camparo

Sample	ccRCC-5	tRCC	tRCC
Gene	*EGFR*	*MET*	*KDR* (VEGFR-2)
Chromosomal location (hg18)	7p12 chr7:55,233,996	7q31 chr7:116,126,445	4q11-12 chr4:55,659,724
CDS Mutation	c.2794C>T	c.71G>A	c.2770C>G
AA Mutation	p.R932C	p.G24E	p.A757G
Protein Domain	Protein Tyrosine Kinase Domain (AA 712-979)	Signal Peptide (AA 1-24)	Extracellular Domain (AA 20-764)
Predicted Functional Impact	high	medium	low
Reads with alternate base pair	245/575 (43%)	46/103 (45%)	27/57 (47%)

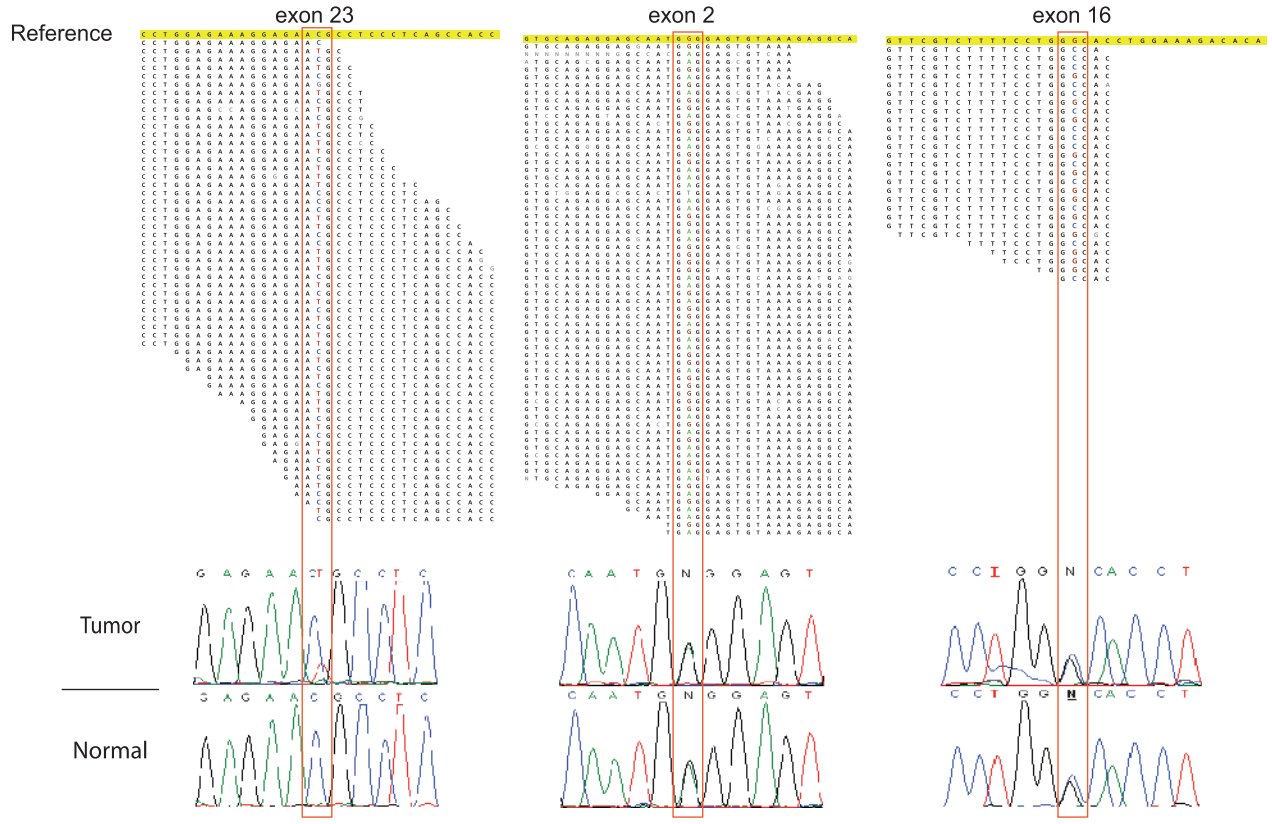

Figure 5. Rare mutations in renal cancer affecting *EGFR*, *MET*, and *KDR*. Three mutations occurring in two RCC samples are given with exact genomic location, base pair, and AA exchange and the percentage of reads that have the mutated allele in the RNA-Seq data. Only the unique reads covering the mutated base are displayed below. Each mutation was evaluated by PCR and conventional Sanger sequencing in tumor and corresponding normal tissue.

et al. appears as a robust signature for *TFE3* tRCC. To further validate specific proteins of this signature, we studied EEF1A2, CNTN3, and MUC1 IHC in several renal cancer subtypes. EEF1A2 is a subunit of the eukaryotic translation elongation factor 1 protein complex delivering tRNA to the ribosome. The alpha 2 isoform is usually expressed in the brain, heart, and skeletal muscle, but high levels are also characteristic for carcinogenesis including breast [36], ovarian [37], and prostate [38] cancers. CNTN3 is the third member of the Contactin family of cell surface proteins. Like Contactins 1 and 2, it is expressed at high levels in the nervous system, but high expression was also found in plasmocytomas [39]. *TFE3* tRCCs underexpress epithelial IHC markers such as MUC1, also known as epithelial membrane antigen (EMA) [40]. Loss of MUC1 is used in addition to TFE3 IHC to support the diagnosis of a translocation carcinoma. However, our data show a significant portion of ccRCC also being negative for MUC1 expression impairing differential diagnosis. IHC for TFE3 protein has proven to be a highly sensitive and specific assay for the *TFE3* tRCC [41], but this assay detects also native TFE3, which is ubiquitously expressed at very low levels. This can lead to false-positive results. In addition, TFE3 IHC is highly dependent on the tissues' formalin fixation. Therefore, the *TFE3* FISH assay is recommended to detect *TFE3* gene rearrangements in cases with equivocal TFE3 IHC results [42]. However, both assays are difficult to interpret when only archival FFPE tissue blocks are available. In the course of our study, we analyzed our cohort of TFE3 immunopositive cases by FISH. Six of 22 (27%) tumors displaying typical histologic features of *TFE3* tRCC had no *TFE3* rearrangements by FISH, which was also confirmed by reanalyzing large sections. Other examples of such RCCs have been reported previously at comparable frequencies [6 of 21 (28%) [7] and 5 of 11 (45%) [30]]. Green et al. [42] suggest the existence of unclassified RCC, which are biologically related to *TFE3* tRCC with TFE3 and cathepsin K expression in the absence of *TFE3* rearrangements. They suspect that other mechanisms than chromosome translocation can affect TFE3 expression. Such a biologic relationship between *TFE3* translocation and TFE3-expressing/non-translocated tumors is supported by our biomarker analysis. Compared to ccRCC, pronounced overexpression of *TMED6-COG8* and EEF1A2 was characteristic for both *TFE3* tRCCs and TFE3-expressing/non-translocated RCCs. Of note though are the differences between *TFE3* translocation and TFE3-expressing/non-translocated tumors regarding CNTN3 and MUC1 expression. We conclude that MUC1 and CNTN3 have limited practical value in routine diagnostics due to the mixed expression pattern in between the spectrum of all tumor subtypes.

The mutations detected in our study occurred in three clinically relevant genes that are rarely affected in RCC and therefore not part of routine diagnostic protocols. All three mutations are unknown in the Catalogue of Somatic Mutations in Cancer and are not listed among the few entries of *EGFR*, *MET*, and *KDR* mutations in RCC samples.

The identified *MET* and *VEGFR2* mutations were both germline and occurred in a *TFE3* tRCC. Germline *MET* mutations are associated with a hereditary form of pRCC hereditary papillary renal carcinoma type 1 (HPRC 1) [43]. Although both mutations separately might not be causal, they might exert synergistic effects on tumor development in this young patient with *TFE3* tRCC. Recently, it has been shown in a phase II trial that germline *MET* mutations in patients with pRCC are highly predictive of response to Foretinib, a drug targeting both MET and VEGFR2 [44]. It remains to be elucidated if *TFE3* tRCCs may be prone to acquire *MET* mutations, and more functional evidence is needed before we can conclude the usefulness of this inhibitor in treating this RCC subtype.

Interestingly, we detected an *EGFR* mutation in one case of ccRCC. Most activating and cancer-driving mutations in *EGFR* are located between exons 18 and 21. The tyrosine kinase domain covers 268 AAs spanning exons 18 to 24; p.R932C is in exon 23; hence, this mutation could be critical. *EGFR* mutations are extremely rare in RCC, and none was found in a series of 63 RCCs [45]. However, this study focused on the hotspot exons 18 to 21 only. To exclude the possibility of hotspot mutations outside exons 18 to 21, we sequenced exons 18 to 23 in 10 *VHL* wild-type ccRCCs from our institute but failed to find more cases with *EGFR* mutations (data not shown).

Mutation detection from next-generation sequencing data is strongly dependent on the mutation type and data quantity and quality. Small insertions/deletions or high GC content might impair the alignment of reads to target genes. Both factors are contributing to the inability to confirm the known *VHL* mutations in our three ccRCC samples (data not shown).

In summary, the application of the FusionSeq algorithm [18] to our RNA-Seq data has proven highly successful in the detection of RNA chimeras and gene fusions in *TFE3* translocation cancer. We obtained new markers for *TFE3* translocation and TFE3-expressing/non-translocated RCCs and identified relevant point mutations.

Acknowledgments

We thank Susanne Dettwiler, André Fitsche, and Giovanna Bosshard for outstanding technical assistance and Eugenia Haralambieva for help with *TFE3* FISH interpretation. We thank the sequencing service of the Institute of Surgical Pathology for performing numerous sequencing reactions.

References

[1] Ross H and Argani P (2010). Xp11 translocation renal cell carcinoma. *Pathology* **42**, 369–373.

[2] Folpe AL and Deyrup AT (2006). Alveolar soft-part sarcoma: a review and update. *J Clin Pathol* **59**, 1127–1132.

[3] Argani P, Aulmann S, Illei PB, Netto GJ, Ro J, Cho HY, Dogan S, Ladanyi M, Martignoni G, Goldblum JR, et al. (2010). A distinctive subset of PEComas harbors TFE3 gene fusions. *Am J Surg Pathol* **34**, 1395–1406.

[4] Antonescu CR, Le Loarer F, Mosquera JM, Sboner A, Zhang L, Chen CL, Chen HW, Pathan N, Krausz T, Dickson BC, et al. (2013). Novel *YAP1-TFE3* fusion defines a distinct subset of epithelioid hemangioendothelioma. *Genes Chromosomes Cancer* **52**, 775–784.

[5] Kim SH, Choi Y, Jeong HY, Lee K, Chae JY, and Moon KC (2011). Usefulness of a break-apart FISH assay in the diagnosis of Xp11.2 translocation renal cell carcinoma. *Virchows Arch* **459**, 299–306.

[6] Macher-Goeppinger S, Roth W, Wagener N, Hohenfellner M, Penzel R, Haferkamp A, Schirmacher P, and Aulmann S (2012). Molecular heterogeneity of TFE3 activation in renal cell carcinomas. *Mod Pathol* **25**, 308–315.

[7] Malouf GG, Monzon FA, Couturier J, Molinié V, Escudier B, Camparo P, Su X, Yao H, Tamboli P, Lopez-Terrada D, et al. (2013). Genomic heterogeneity of translocation renal cell carcinoma. *Clin Cancer Res* **19**, 4673–4684.

[8] Mosquera JM, Dal Cin P, Mertz KD, Perner S, Davis IJ, Fisher DE, Rubin MA, and Hirsch MS (2011). Validation of a TFE3 break-apart FISH assay for Xp11.2 translocation renal cell carcinomas. *Diagn Mol Pathol* **20**, 129–137.

[9] Berger MF, Lawrence MS, Demichelis F, Drier Y, Cibulskis K, Sivachenko AY, Sboner A, Esgueva R, Pflueger D, Sougnez C, et al. (2011). The genomic complexity of primary human prostate cancer. *Nature* **470**, 214–220.

[10] Campbell PJ, Yachida S, Mudie LJ, Stephens PJ, Pleasance ED, Stebbings LA, Morsberger LA, Latimer C, McLaren S, Lin ML, et al. (2010). The patterns and dynamics of genomic instability in metastatic pancreatic cancer. *Nature* **467**, 1109–1113.

[11] Berger MF, Levin JZ, Vijayendran K, Sivachenko A, Adiconis X, Maguire J, Johnson LA, Robinson J, Verhaak RG, Sougnez C, et al. (2010). Integrative analysis of the melanoma transcriptome. *Genome Res* **20**, 413–427.

[12] Maher CA, Palanisamy N, Brenner JC, Cao X, Kalyana-Sundaram S, Luo S, Khrebtukova I, Barrette TR, Grasso C, Yu J, et al. (2009). Chimeric transcript discovery by paired-end transcriptome sequencing. *Proc Natl Acad Sci USA* **106**, 12353–12358.

[13] Pflueger D, Terry S, Sboner A, Habegger L, Esgueva R, Lin PC, Svensson MA, Kitabayashi N, Moss BJ, MacDonald TY, et al. (2011). Discovery of non-ETS gene fusions in human prostate cancer using next-generation RNA sequencing. *Genome Res* **21**, 56–67.

[14] Guo G, Gui Y, Gao S, Tang A, Hu X, Huang Y, Jia W, Li Z, He M, Sun L, et al. (2012). Frequent mutations of genes encoding ubiquitin-mediated proteolysis pathway components in clear cell renal cell carcinoma. *Nat Genet* **44**, 17–19.

[15] Varela I, Tarpey P, Raine K, Huang D, Ong CK, Stephens P, Davies H, Jones D, Lin ML, Teague J, et al. (2011). Exome sequencing identifies frequent mutation of the SWI/SNF complex gene *PBRM1* in renal carcinoma. *Nature* **469**, 539–542.

[16] Cancer Genome Atlas Research Network (2013). Comprehensive molecular characterization of clear cell renal cell carcinoma. *Nature* **499**, 43–49.

[17] Camparo P, Vasiliu V, Molinie V, Couturier J, Dykema KJ, Petillo D, Furge KA, Comperat EM, Lae M, Bouvier R, et al. (2008). Renal translocation carcinomas: clinicopathologic, immunohistochemical, and gene expression profiling analysis of 31 cases with a review of the literature. *Am J Surg Pathol* **32**, 656–670.

[18] Sboner A, Habegger L, Pflueger D, Terry S, Chen DZ, Rozowsky JS, Tewari AK, Kitabayashi N, Moss BJ, Chee MS, et al. (2010). FusionSeq: a modular framework for finding gene fusions by analyzing paired-end RNA-sequencing data. *Genome Biol* **11**, R104.

[19] Bruder E, Moch H, Ehrlich D, Leuschner I, Harms D, Argani P, Briner J, Graf N, Selle B, Rufle A, et al. (2007). Wnt signaling pathway analysis in renal cell carcinoma in young patients. *Mod Pathol* **20**, 1217–1229.

[20] Bruder E, Passera O, Harms D, Leuschner I, Ladanyi M, Argani P, Eble JN, Struckmann K, Schraml P, and Moch H (2004). Morphologic and molecular characterization of renal cell carcinoma in children and young adults. *Am J Surg Pathol* **28**, 1117–1132.

[21] Mertz KD, Demichelis F, Kim R, Schraml P, Storz M, Diener PA, Moch H, and Rubin MA (2007). Automated immunofluorescence analysis defines microvessel area as a prognostic parameter in clear cell renal cell cancer. *Hum Pathol* **38**, 1454–1462.

[22] Habegger L, Sboner A, Gianoulis TA, Rozowsky J, Agarwal A, Snyder M, and Gerstein M (2011). RSEQtools: a modular framework to analyze RNA-Seq data using compact, anonymized data summaries. *Bioinformatics* **27**, 281–283.

[23] Mortazavi A, Williams BA, McCue K, Schaeffer L, and Wold B (2008). Mapping and quantifying mammalian transcriptomes by RNA-Seq. *Nat Methods* **5**, 621–628.

[24] Dalgliesh GL, Furge K, Greenman C, Chen L, Bignell G, Butler A, Davies H, Edkins S, Hardy C, Latimer C, et al. (2010). Systematic sequencing of renal carcinoma reveals inactivation of histone modifying genes. *Nature* **463**, 360–363.

[25] Kircher M, Stenzel U, and Kelso J (2009). Improved base calling for the Illumina Genome Analyzer using machine learning strategies. *Genome Biol* **10**, R83.

[26] Rechsteiner MP, von Teichman A, Nowicka A, Sulser T, Schraml P, and Moch H (2011). *VHL* gene mutations and their effects on hypoxia inducible factor HIFα: identification of potential driver and passenger mutations. *Cancer Res* **71**, 5500–5511.

[27] Bode B, Frigerio S, Behnke S, Senn B, Odermatt B, Zimmermann DR, and Moch H (2006). Mutations in the tyrosine kinase domain of the *EGFR* gene are rare in synovial sarcoma. *Mod Pathol* **19**, 541–547.

[28] Argani P, Olgac S, Tickoo SK, Goldfischer M, Moch H, Chan DY, Eble JN, Bonsib SM, Jimeno M, Lloreta J, et al. (2007). Xp11 translocation renal cell carcinoma in adults: expanded clinical, pathologic, and genetic spectrum. *Am J Surg Pathol* **31**, 1149–1160.

[29] Martignoni G, Gobbo S, Camparo P, Brunelli M, Munari E, Segala D, Pea M, Bonetti F, Illei PB, Netto GJ, et al. (2011). Differential expression of cathepsin K in neoplasms harboring *TFE3* gene fusions. *Mod Pathol* **24**, 1313–1319.

[30] Zhong M, De Angelo P, Osborne L, Paniz-Mondolfi AE, Geller M, Yang Y, Linehan WM, Merino MJ, Cordon-Cardo C, and Cai D (2012). Translocation renal cell carcinomas in adults: a single-institution experience. *Am J Surg Pathol* **36**, 654–662.

[31] Tanaka M, Kato K, Gomi K, Matsumoto M, Kudo H, Shinkai M, Ohama Y, Kigasawa H, and Tanaka Y (2009). Perivascular epithelioid cell tumor with SFPQ/PSF-TFE3 gene fusion in a patient with advanced neuroblastoma. *Am J Surg Pathol* **33**, 1416–1420.

[32] Maher CA, Kumar-Sinha C, Cao X, Kalyana-Sundaram S, Han B, Jing X, Sam L, Barrette T, Palanisamy N, and Chinnaiyan AM (2009). Transcriptome sequencing to detect gene fusions in cancer. *Nature* **458**, 97–101.

[33] Rickman DS, Pflueger D, Moss B, VanDoren VE, Chen CX, de la Taille A, Kuefer R, Tewari AK, Setlur SR, Demichelis F, et al. (2009). SLC45A3-ELK4 is a novel and frequent erythroblast transformation-specific fusion transcript in prostate cancer. *Cancer Res* **69**, 2734–2738.

[34] Wang X, Yang R, Jadhao SB, Yu D, Hu H, Glynn-Cunningham N, Sztalryd C, Silver KD, and Gong DW (2012). Transmembrane emp24 protein transport domain 6 is selectively expressed in pancreatic islets and implicated in insulin secretion and diabetes. *Pancreas* **41**, 10–14.

[35] Smith RD and Lupashin VV (2008). Role of the conserved oligomeric Golgi (COG) complex in protein glycosylation. *Carbohydr Res* **343**, 2024–2031.

[36] Tomlinson VA, Newbery HJ, Wray NR, Jackson J, Larionov A, Miller WR, Dixon JM, and Abbott CM (2005). Translation elongation factor eEF1A2 is a potential oncoprotein that is overexpressed in two-thirds of breast tumours. *BMC Cancer* **5**, 113.

[37] Tomlinson VA, Newbery HJ, Bergmann JH, Boyd J, Scott D, Wray NR, Sellar GC, Gabra H, Graham A, Williams AR, et al. (2007). Expression of eEF1A2 is associated with clear cell histology in ovarian carcinomas: overexpression of the gene is not dependent on modifications at the EEF1A2 locus. *Br J Cancer* **96**, 1613–1620.

[38] Scaggiante B, Dapas B, Bonin S, Grassi M, Zennaro C, Farra R, Cristiano L, Siracusano S, Zanconati F, Giansante C, et al. (2012). Dissecting the expression of *EEF1A1/2* genes in human prostate cancer cells: the potential of EEF1A2 as a hallmark for prostate transformation and progression. *Br J Cancer* **106**, 166–173.

[39] Shimoda Y and Watanabe K (2009). Contactins: emerging key roles in the development and function of the nervous system. *Cell Adh Migr* **3**, 64–70.

[40] Argani P, Antonescu CR, Illei PB, Lui MY, Timmons CF, Newbury R, Reuter VE, Garvin AJ, Perez-Atayde AR, Fletcher JA, et al. (2001). Primary renal neoplasms with the *ASPL-TFE3* gene fusion of alveolar soft part sarcoma: a distinctive tumor entity previously included among renal cell carcinomas of children and adolescents. *Am J Pathol* **159**, 179–192.

[41] Argani P, Lal P, Hutchinson B, Lui MY, Reuter VE, and Ladanyi M (2003). Aberrant nuclear immunoreactivity for TFE3 in neoplasms with TFE3 gene fusions: a sensitive and specific immunohistochemical assay. *Am J Surg Pathol* **27**, 750–761.

[42] Green WM, Yonescu R, Morsberger L, Morris K, Netto GJ, Epstein JI, Illei PB, Allaf M, Ladanyi M, Griffin CA, et al. (2013). Utilization of a TFE3 break-apart FISH assay in a renal tumor consultation service. *Am J Surg Pathol* **37**, 1150–1163.

[43] Schmidt L, Duh FM, Chen F, Kishida T, Glenn G, Choyke P, Scherer SW, Zhuang Z, Lubensky I, Dean M, et al. (1997). Germline and somatic mutations in the tyrosine kinase domain of the MET proto-oncogene in papillary renal carcinomas. *Nat Genet* **16**, 68–73.

[44] Choueiri TK, Vaishampayan U, Rosenberg JE, Logan TF, Harzstark AL, Bukowski RM, Rini BI, Srinivas S, Stein MN, Adams LM, et al. (2013). Phase II and biomarker study of the dual MET/VEGFR2 inhibitor foretinib in patients with papillary renal cell carcinoma. *J Clin Oncol* **31**, 181–186.

[45] Minner S, Rump D, Tennstedt P, Simon R, Burandt E, Terracciano L, Moch H, Wilczak W, Bokemeyer C, Fisch M, et al. (2012). Epidermal growth factor receptor protein expression and genomic alterations in renal cell carcinoma. *Cancer* **118**, 1268–1275.